Translational Oncology 28 (2023) 101616

Contents lists available at ScienceDirect

Translational Oncology

journal homepage: www.elsevier.com/locate/tranon

Original Research

The clinical application of ^{68}Ga-PSMA PET/CT and regulating mechanism of PSMA expression in patients with brain metastases of lung cancer

Yuchen Pei [a,2], Chang Liu [b,2], Mingtao Feng [c], Liangdong Li [c], Changshuai Zhou [c], Lei Chen [c], Xin Hu [a,1], Shaoli Song [b,1], Yiqun Cao [c,1], Yang Gao [c,1,*]

[a] Precision Cancer Medicine Center, Fudan University Shanghai Cancer Center, Shanghai, China
[b] Department of Nuclear Medicine, Fudan University Shanghai Cancer Center, Shanghai, China
[c] Department of Neurosurgery, Fudan University Shanghai Cancer Center, Shanghai, China

ARTICLE INFO

Keywords:
Brain metastases
Lung cancer
PSMA PET/CT
Immunohistochemistry
Single-cell RNA sequencing

ABSTRACT

Brain metastases (BMs) of lung cancer are common malignant intracranial tumours associated with severe neurological symptoms and an abysmal prognosis. Prostate-specific membrane antigen (PSMA) has been reported to express significantly in a variety of solid tumours. However, the clinical applications of ^{68}Ga-PSMA PET/CT and the mechanism of PSMA expression in patients with BMs of lung cancer have rarely been reported. Experiments with ^{68}Ga-PSMA PET/CT and immunohistochemical staining were conducted to evaluate the expression of PSMA from seven patients with BMs of lung cancer who accepted surgical treatment in Fudan University Shanghai Cancer Center between October 2020 and October 2021. The mechanism of PSMA expression in BMs of lung cancer was explored by using single-cell RNA sequencing. The median maximum standardized uptake value (SUVmax) in BMs was higher than that in primary lung cancer (8.6 ± 2.8 vs. 3.6 ± 1.3, $P < 0.01$). The mean SUVmax in BMs was 1.76-fold higher than that in the liver, which indicated the potential of PSMA radioligand therapy (PSMA-RLT) for BMs. BMs showed intense PSMA staining, while normal lung tissue had no PSMA staining and there was only faint primary lung cancer staining by immunohistochemistry (IHC). Single-cell RNA sequencing (scRNA-seq) analysis found that PSMA was mainly expressed in oligodendrocytes of BMs, whereas it was expressed at lower levels in solid cells of lung cancer. PSMA expression in oligodendrocytes might be regulated by the factors ATF3 and NR4A1, which were associated with ER stress.

1. Introduction

Brain metastases (BMs) of solid tumours are the most frequent intracranial tumours, approximately 10-fold more common than primary brain tumours [1]. BMs are associated with severe neurological symptoms and an abysmal prognosis compared to other metastatic sites. Lung cancer is the common primary tumour with BMs and more than 50% of total lung cancer develop BMs [2]. Although various therapeutic approaches, such as surgery, radiotherapy and immunotherapy, have been used for the treatment of lung cancer associated with BMs, its poor response is still essential issues that need to be urgently solved [3].

Prostate-specific membrane antigen (PSMA), also known as glutamate carboxypeptidase II (GCPII) or N-acetyl-aspartyl-glutamate (NAAG) peptidase, is a transmembrane glycoprotein encoded by the *folh1* gene [4]. PSMA is the major enzyme that hydrolyses the neurotransmitter NAAG (N-acetyl-aspartyl-glutamate) to NAA and free glutamate, and it could be targeted to treat several neurological disorders, including stroke, traumatic brain injury and schizophrenia [5]. PSMA is highly expressed in prostate cancers and is positively correlated with the growth and invasiveness of these tumours [6,7]. Notably, many

Abbreviations: BMs, Brain metastases; PSMA, Prostate-specific membrane antigen; PSME, PSMA enhancer; SUVmax, The median standardized uptake value; PSMA-RLT, PSMA radioligand therapy; IHC, Immunohistochemistry; scRNA-seq, Single-cell RNA sequencing; ER, Endoplasmic reticulum; GCPII, Glutamate carboxypeptidase II; NAAG, N-acetyl-aspartyl-glutamate; GBM, Glioblastoma multiforme; NSCLC, Non-small cell lung cancer; GO, Gene Ontology; KEGG, Kyoto Encyclopedia of Genes and Genomes; SCLC, Small cell lung cancer; PSMA ADCs, PSMA antibody–drug conjugates.

* Corresponding author.
E-mail address: baiyizhanshi@126.com (Y. Gao).
[1] These authors contributed equally to this work.
[2] Yuchen Pei and Chang Liu are co-first authors.

https://doi.org/10.1016/j.tranon.2023.101616
Received 21 July 2022; Received in revised form 18 October 2022; Accepted 2 January 2023

studies have reported that PSMA not just expressed in prostate cancer cells but also expressed in neovascular endothelial cells of various cancers, including glioblastoma, lung cancer, and breast cancer [8–10].

Recent studies evaluating the efficacy of ^{177}Lu-PSMA radioligand therapy (PSMA-RLT) demonstrated favourable results in prostate cancer patients [11]. In glioblastoma multiforme (GBM), a total of 32 GBM specimens displayed positive PSMA staining, and the anti-PSMA antibody (J591) performed well in targeting the neovasculature of non-prostate malignancies *in vivo* [12]. Therefore, PSMA could be a potential therapeutic target in multiple types of cancers [13,14].

PSMA is highly expressed in neovasculature of non-small cell lung cancer (NSCLC) with higher tumour grading (G3/G4) and might be associated with brain metastases of lung carcinomas [10]. However, few reports have applied PSMA PET/CT to assess the expression of PSMA in patients with BMs of lung cancer, let alone the mechanism of PSMA expression in secondary brain tumours.

In this study, we evaluated the clinical application of ^{68}Ga-PSMA PET/CT in patients with BMs of lung cancer. In addition, the expression and mechanism of PSMA in BMs were also investigated by using PET/CT images, immunohistochemistry (IHC) and single-cell RNA sequencing (scRNA-seq) data.

2. Materials and methods

2.1. Clinical characteristics

A total of seven patients with BMs of lung cancer who accepted surgical treatment at Fudan University Shanghai Cancer Center between October 2020 and October 2021 were included in this study. Age, sex, maximum standardized uptake value (SUVmax), and IHC features were analysed. All patients provided informed consent. Ethical approval for this study was obtained from the ethics committee of the Fudan University Shanghai Cancer Center.

2.2. PSMA-targeted imaging modalities

^{68}Ga-PSMA PET/CT scans were obtained comply with the international guidelines [15]. Briefly, the routine scan was initiated 60 min after administration of the tracer (3.7 MBq/kg). ^{68}Ga-PSMA-11 PET/CT did not require fasting. PET/CT scans were performed using a Siemens mCT Flow PET/CT scanner (Siemens Healthcare, Knoxville, Tennessee, USA). A non-contrast-enhanced CT scan was performed using the following parameters: slice thickness of 3 mm, increment of 2 mm, soft tissue reconstruction kernel, 120 keV. Immediately after CT scanning, a whole-body PET (from the level of the skull base to the knee) was acquired in 3-D (matrix 200 × 200). A lesion-by-lesion analysis was performed using PET/CT volume computer-assisted reading workstation (Syngo; Siemens Healthcare).

2.3. Immunohistochemical staining assay

Patient tissue samples were embedded in paraffin, deparaffinized with xylene, rehydrated with gradient concentrations of alcohol and washed with PBS. EDTA antigen repair buffer was utilized to immerse the sections, which were then boiled for 30 min. After washing with PBS, each section was blocked with hydrogen peroxide for 25 min. Then, the sections were incubated with 3% BSA for 30 min. Primary anti-PSMA antibodies (ab19071, 1:100, Abcam, UK) were incubated with the sections at 4 ℃ overnight. Then, the secondary antibody streptomycin-HRP was added and incubated with the sections at room temperature for 1 h after washing. The sections were coloured with DAB and stained with 10% Harris haematoxylin for 3 min. Then, the slides were dehydrated with gradient alcohol and sealed with neutral balsam. Images of the slides were analysed with a microscope (OLYMPUS) and ImageJ software. The extent of PSMA staining in each immune-stained section was scored by an expert neuropathologist as follows: less than 5% staining (none, ±), 6% to 25% staining (minimal, +), 26% to 50% staining (moderate, ++), 51% to 75% staining (strong, +++), and 76% to 100% staining (very strong, ++++).

2.4. Single-cell RNA sequencing analysis

The single-cell matrix was accessed from the NCBI Gene Expression Omnibus database (accession code GSE131907), including the corresponding annotation [16]. The R package Seurat was used to perform tSNE dimension reduction and visualization. First, the data were normalized by the function in the Seurat package. Then, PCA was implemented for preliminary dimension reduction with the function RunPCA. The functions named FindNeighbours and FindClusters were used to prepare for the tSNE analysis, and then we used RunTSNE to acquire the clustering results. Then, the folh1 violin plot was outputted by VlnPlot. For selecting the marker genes, the natural logarithms of fold change greater than 0.5 and adjusted P value less than 0.05 were defined as significantly expressing genes. Subsequently, the obvious differences among the top 20 genes were selected in each cluster by the function DimHeatmap.

2.5. Pathway enrichment analysis

The significantly expressed genes in the cluster of interest were selected for enrichment analysis. After gene list preparation, gene symbols were converted to ENTREZID by the function named bitr in the R package clusterProfiler. Then, the selected genes were categorized according to the functional gene sets in the Gene Ontology (GO) and Kyoto Encyclopedia of Genes and Genomes (KEGG) databases. Finally, the enriched pathway was plotted by the function barplot.

2.6. Immunofluorescence staining assay

Patient tissue samples were fixed, embedded in paraffin, cleared in xylene for 20 min and then immersed for 1 min each in absolute ethanol, 95% ethanol, and 70% ethanol. Then, 100 μl hydrogen peroxide blocking solution was added and incubated at room temperature for 10 min after washing with water for 5 min. After washing with PBS 3 times, 100 μl 5% BSA was added to each section for 20 min at room temperature, and then the sections were incubated with anti-PSMA antibodies (ab133579, 1:400, Abcam, UK) and anti-oligo antibodies (ab109186, 1:200, Abcam, UK) at 4 ℃ overnight. After washing with PBS 3 times, the sections were incubated with secondary antibodies (ab205718, 1:1000, Abcam, UK) conjugated to Try-488 (Runnerbio, Shanghai, China) for 30 min. Then, the same procedure was repeated to stain the oligodendrocytes with Try-cy3 (Runnerbio, Shanghai, China).

2.7. Statistical analysis

Data were expressed as the mean ± SD. The differences between groups were determined with Student's *t test*. GraphPad Prism 8.0 Software and Seurat were used. The R packages Seurat and clusterProfiler were used for scRNA-seq analysis. The P value less than 0.05 was considered statistically significant.

3. Results

3.1. PSMA is overexpressed in lung cancer associated with BMs

This study included seven male patients with a median age of 63.7 years (ranging from 43 to 76 years). There was one small cell lung cancer (SCLC) and six NSCLC associated with BMs. All PET/CTs clearly depicted PSMA ligand uptake in areas of the primary lung cancer and BMs (Table 1).

According to the ^{68}Ga-PSMA-PET/CT images of the seven patients, the uptake of ^{68}Ga-PSMA was increased in BMs compared to that in

Table 1
Summary of PSMA expression and ^{68}Ga-PSMA PET/CT imaging in seven patients with BMs of lung cancer.

No.	Gender	Age	Pathology	Primary lung cancer		BMs[3]		Liver background	BMs/Liver ratio (SUVmax)
				SUVmax[1]	IHC[2]	SUVmax	IHC	SUVmax	
1	Male	62	SCLC[4]	4.1	+	13.8	+++	6.1	2.26
2	Male	58	NSCLC[5]	3.9	+	6.7	++	4.3	1.56
3	Male	69	NSCLC	5.6	+	5.6	++	3.5	1.60
4	Male	43	NSCLC	2.1	±	10.7	+++	5.1	2.10
5	Male	76	NSCLC	3.3	±	7.6	++	4.7	1.62
6	Male	65	NSCLC	4.5	+	8.6	+++	5.5	1.56
7	Male	73	NSCLC	1.8	±	7.3	++	4.5	1.62
Average (range)		63.7 (43 - 76)		3.6 (1.8 - 5.6)		8.6 (5.6 - 13.8)		4.8 (3.5 - 6.1)	1.76 (1.56 - 2.26)

[1] SUVmax: maximum standardized uptake value.
[2] IHC: immunohistochemistry.
[3] BMs: brain metastases.
[4] SCLC: small cell lung cancer.
[5] NSCLC: non-small cell lung cancer. All the NSCLC are adenocarcinoma.

primary lung cancer (Fig. 1A). The SUVmax values ranged from 1.8 to 5.6 in primary lung cancer and ranged from 5.6 to 13.8 in BMs. The mean SUVmax was 3.6 ± 1.3 in primary lung cancer and 8.6 ± 2.8 in BMs ($p = 0.0073$) (Fig. 1B). The mean SUVmax in BMs was 1.76-fold higher than that in the liver, which indicated the potential of PSMA-RLT for detecting BMs (Table 1). In addition, the uptake value of PSMA in BMs of SCLC was significantly higher than that in BMs of NSCLC (Table 1). The imaging modalities indicated that the expression of PSMA had a different behaviour when BMs occurred. As shown in Fig. 1C, BMs showed intense PSMA staining, while normal lung tissue had no PSMA staining and there was only faint primary lung cancer staining on IHC. The more extensive staining of PSMA was present on IHC, the higher uptake of PSMA was shown on PET/CT imaging. Interestingly, PSMA in BMs was expressed not only in blood vessels but also in solid regions.

3.2. *PSMA is significantly overexpressed in oligodendrocytes of BMs*

To investigate the expression of PSMA in the solid regions of BMs, we analysed scRNA-seq data from GSE131907, which included cells derived from normal lung tissues, primary tumour sites and BMs of 44 lung cancer patients. We found that PSMA (folh1) was hardly expressed in normal lung cells and only faintly expressed in primary lung tumour cells (Fig. 2A,B). However, in BMs, PSMA was highly expressed in oligodendrocytes (Fig. 2C). It is an unprecedented finding that oligodendrocytes infiltrated in BMs of lung cancers and highly expressed PSMA. The expression of PSMA was higher in BMs than that in primary lung cancer, which is consistent with the results of the PSMA PET/CT imaging and IHC.

3.3. *Immunofluorescence staining confirmed the expression of PSMA in BMs*

Immunofluorescence staining was performed to confirm whether oligodendrocytes infiltrating into the BMs of lung cancer could express PSMA. As expected, the localization of PSMA and oligodendrocytes were overlapped in BMs of lung cancer (Fig. 3). This interesting phenomenon prompted us to investigate the mechanism of PSMA expression in oligodendrocytes, which might be a potential therapeutic target for BMs of lung cancer.

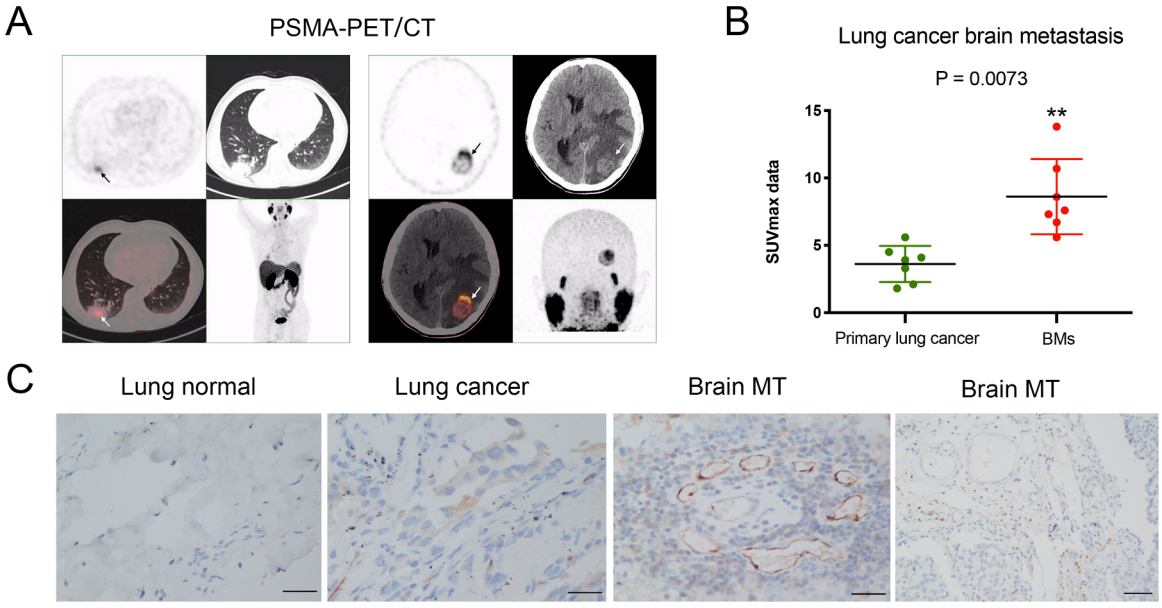

Fig. 1. The expression of PSMA prostate-specific membrane antigen (PSMA) in brain metastases (BMs) of lung cancer. (A) Increased uptake of ^{68}Ga-PSMA was observed in BMs. (B) The BMs showed significantly increased SUVmax values compared with primary lung cancer ($P < 0.01$). (C) PSMA staining was intense in BMs, including blood vessels and solid cells (×200).

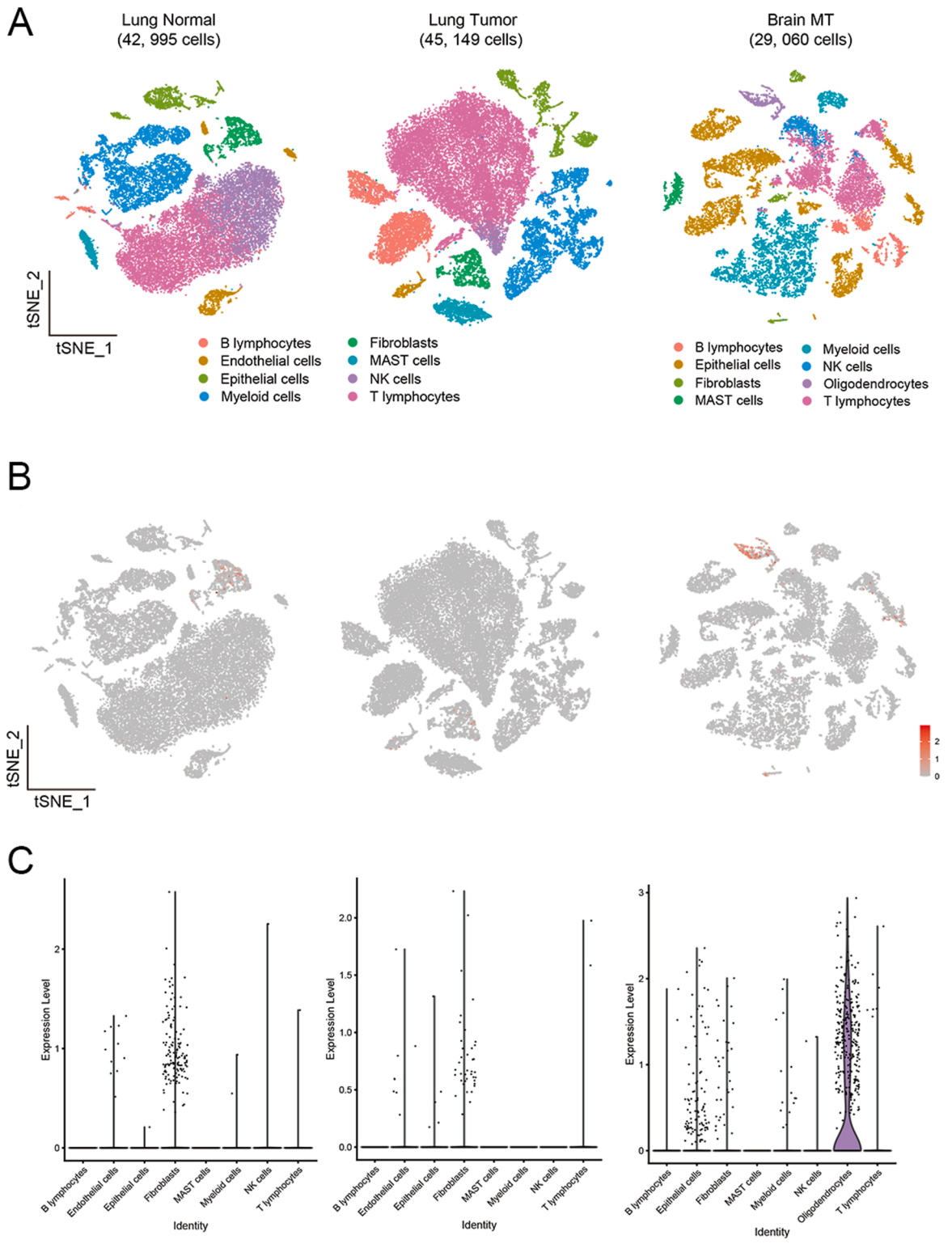

Fig. 2. FOLH1 is highly expressed in oligodendrocytes. (A) tSNE projection within three origins, coloured by cell types from the three origins. (B) BMs have intense PSMA expression, while normal lung tissue and primary lung cancer have faint PSMA expression. (C) Violin plot showing that PSMA is highly expressed in oligodendrocytes of BMs and expressed at low levels in normal and tumour lung cells.

3.4. The expression of PSMA might be associated with ER stress

We used scRNA-seq data to elucidate the underlying biological process of PSMA expression in brain metastases. A total of 716 oligodendrocytes in brain cells were selected, and six clusters were obtained from this analysis (Fig. 4A). The folh1 gene was extensively expressed in oligodendrocytes of cluster 3 (Fig. 4B,C). Indeed, the expression of PSMA in oligodendrocytes revealed its close association with several pathways in oligodendrocytes infiltrating BMs. The results of GO and KEGG signalling pathway enrichment suggested that biological processes such as the unfolded protein response and protein processing in the ER were significantly enriched when PSMA was upregulated in BMs

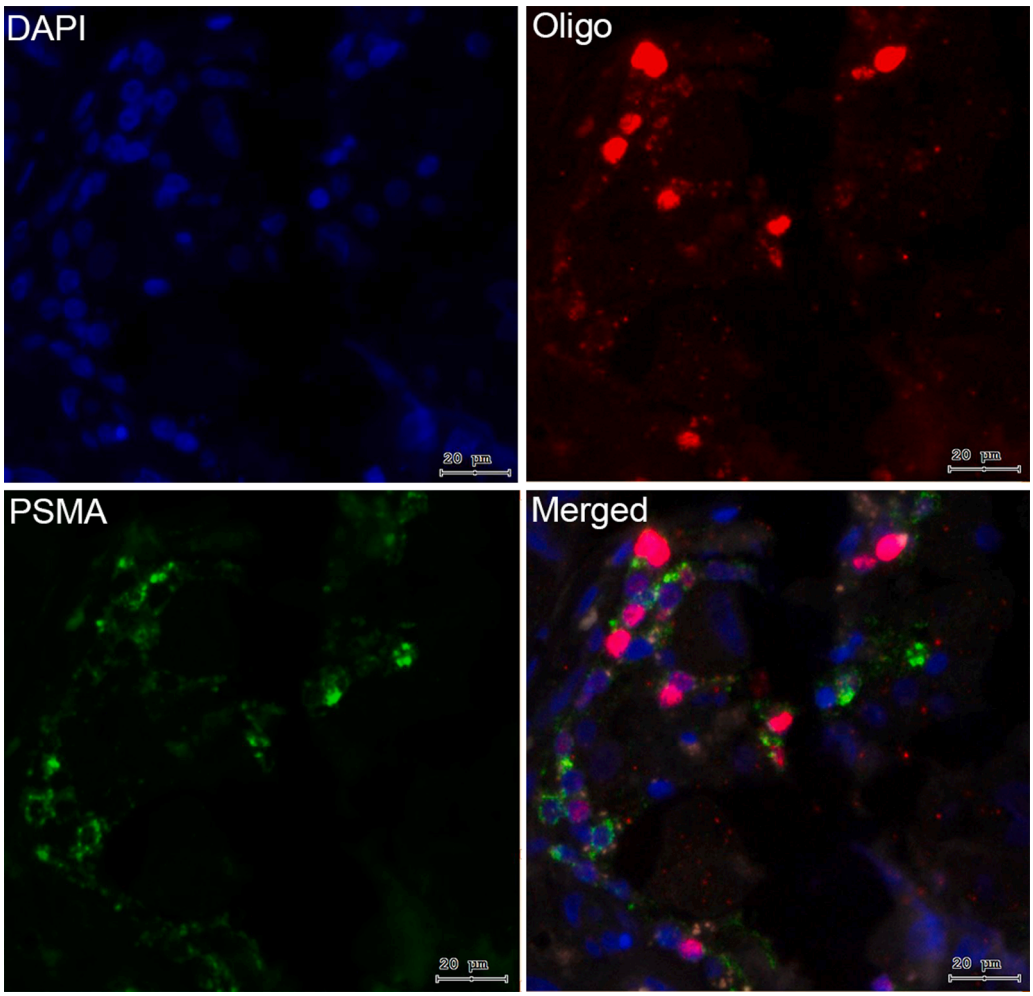

Fig. 3. FOLH1 is significantly expressed in oligodendrocytes of BMs. Immunofluorescence staining to identify the cells that overexpress PSMA in BMs. The top left column shows the cell nucleus in blue by 4′,6-diamidino-2-phenylindole (DAPI); The top right column shows oligodendrocytes stained. The third column shows PSMA stained, and the final column a merged image of the three channels.

(Fig. 4D). The expression of PSMA might be associated with ER stress, which needs to be confirmed by additional experiments.

3.5. Transcription factors ATF3 and NR4A1 regulated the expression of PSMA

To investigate the mechanism of PSMA expression in oligodendrocytes of BMs, we focused on cluster 3, which had the highest level of folh1 expression among the six clusters (Fig. 5A). We noticed that the transcription factors ATF3 and NR4A1 in cluster 3 predominantly bound to the PSMA promoter region, which was investigated by the JASPAR website (Fig. 5B). Altogether, these results suggested that ATF3 and NR4A1 might bind to the promoter region of folh1, regulating the overexpression of PSMA in oligodendrocytes.

4. Discussion

PSMA is highly expressed in the endothelial cells of blood vessels and promotes neovascularization in solid cancers [8,17–18]. In our preliminary observations, PSMA promoted neovascularization in GBM by interacting with ITGB4 and regulating the NF-κB signalling pathway [8]. PSMA probably affects the secretion of matrix metalloproteinase (MMP) in invasive tumours, decreases the basement membrane and extracellular matrix and promotes tumour invasiveness in prostate cancers [19]. PSMA plays an important role in the promotion of tumour development and might be a diagnostic and therapeutic target in various cancers.

PSMA PET/CT, due to its excellent specificity, has a wide range of applications in prostate cancer, including guiding biopsies, surgery and radiotherapy [20]. In recent years, researchers have used ^{68}Ga-PSMA PET/CT to assess the diagnosis, recurrence, and progression of glioblastoma [21]. Although PSMA has been used in several types of cancers as a new imaging modality, few studies have focused on BMs of lung cancer. The reported SUVmax of lung cancer ranged from 4.8 to 5.6, while SUVmax ranged from 3.7 to 7.0 in nine patients with NSCLC [11]. However, the literature on PSMA tracer uptake by lung cancer derives from accidental findings when patients receive PSMA PET/CT imaging for their prostate cancer. There is a lack of reports on the uptake of PSMA PET/CT in lung cancer associated with BMs. Hence, we used ^{68}Ga-PSMA PET/CT to detect BMs of lung cancer in seven patients. Interestingly, we found increased uptake of ^{68}Ga-PSMA in BMs compared to primary lung cancer. The SUVmax values ranged from 1.8 to 5.6 in primary cancer and ranged from 5.6 to 13.8 in BMs. In addition, the uptake value of PSMA in BMs from SCLC was significantly higher than that in BMs from NSCLC. PSMA PET/CT is expected to be useful in the diagnosis and monitoring the treatment response of lung cancer associated with BMs.

Since PSMA-RLT demonstrated remarkable therapeutic efficacy in prostate cancer, it is anticipated that PSMA-RLT could be applied to other solid cancers. Positive treatment outcomes were reported for PSMA-RLT (^{177}Lu-/^{68}Ga-PSMA) in some studies, including salivary gland cancer, thyroid cancer, and glioblastoma [22–24]. Importantly,

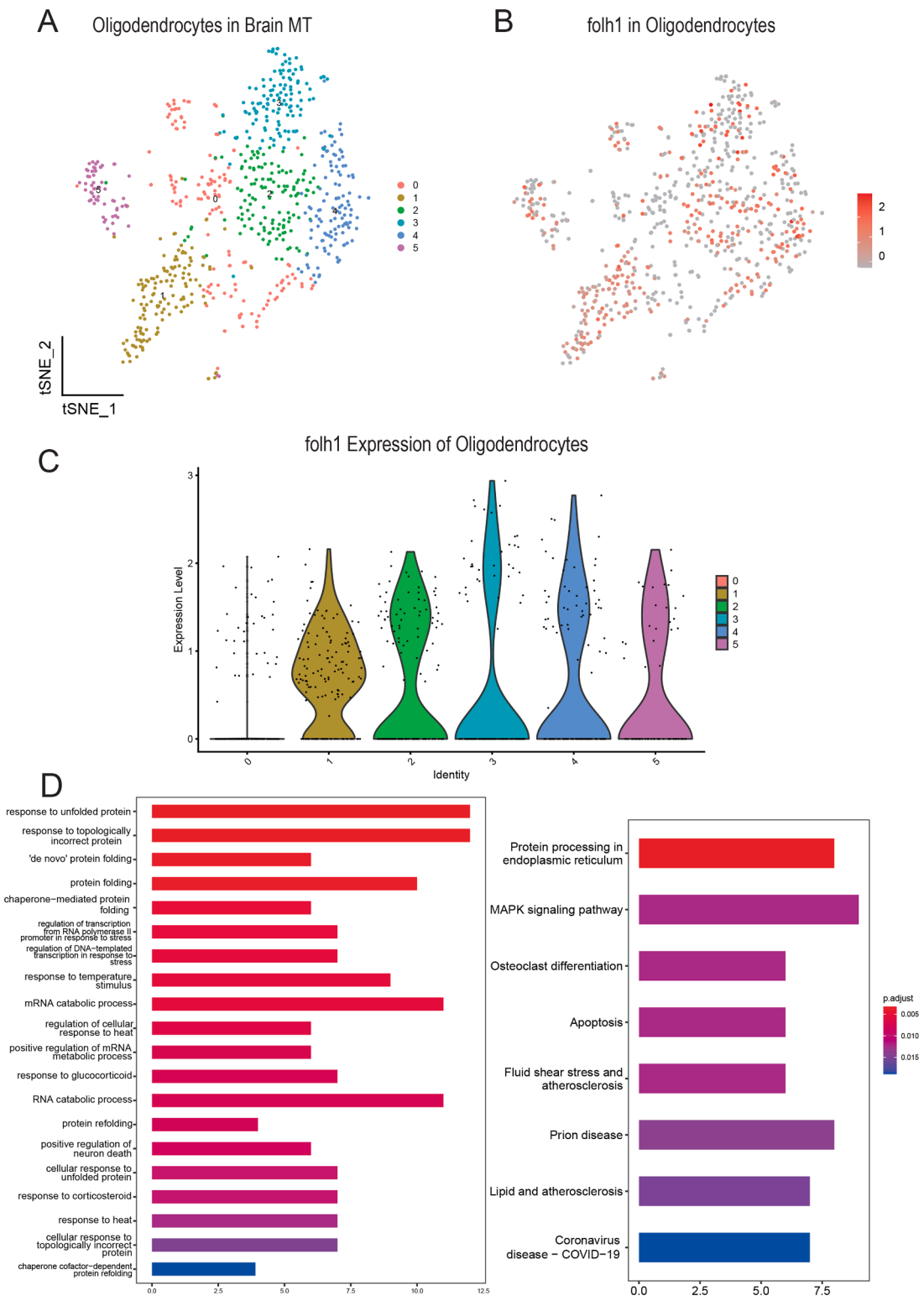

Fig. 4. The expression of PSMA associated with ER stress. (A) tSNE projection was implemented to explore folh1 expression in all oligodendrocytes (coloured to indicate 6 clusters). (B) tSNA projection was performed to present the levels of folh1 (red means a high level of folh 1, grey means no expression). (C) A violin plot quantifying folh1 expression in 6 clusters. (D) The enrichment analysis based on GO and KEGG signalling pathways identified in Cluster 3.

the treatment was generally well tolerated, with no or only low-grade adverse events. PSMA-RLT eligibility in prostate cancer is assessed through PSMA PET/CT imaging (cut-off tumour/liver ratio > 1.5) according to the EANM guidelines [25]. It is worth noting that there are essential differences between prostate cancer and solid cancers because of their heterogeneous radiosensitivity. Lung cancer is generally radiosensitive, and the mean SUVmax of BMs was 1.76-fold higher than that in the liver in our study, which indicated that PSMA-RLT treatment might be feasible in patients with BMs of lung cancer based on their high PSMA tracer uptake.

Regarding PSMA IHC, the expression level of PSMA in the neovasculature of primary lung cancer ranged from 45% in adenocarcinoma

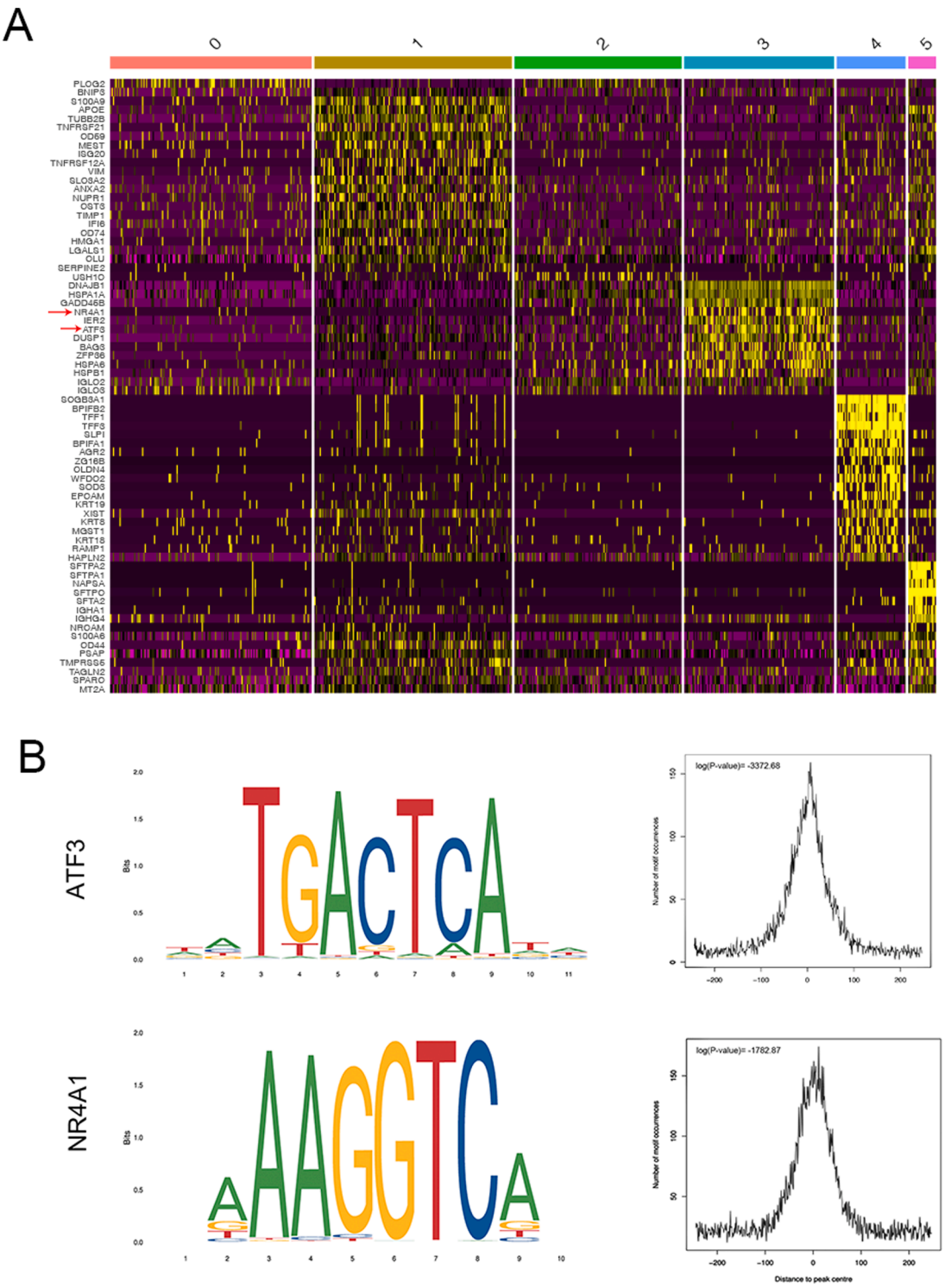

Fig. 5. Transcription factors ATF3 and NR4A1 regulate PSMA expression. (A) Heatmap of marker genes in 6 clusters. (B) Motif prediction of ATF3 and NR4A1 binding to the promoter of the folh1 gene.

to 70% in large cell carcinoma and SCLC [10,26]. In our study, all primary lung cancers, as well as in BMs, showed positive PSMA staining on IHC. BMs showed intense PSMA staining, while normal lung tissue had no PSMA staining and primary lung cancer had only faint staining. Of course, the staining results of PSMA are affected by the staining procedure, antibody concentration, specimen quality, pathologist experience, etc. Positive staining of the tumour cells was shown in all subtypes of NSCLC but not in SCLC [26]. Other researchers reported that a fraction of NSCLC cases had PSMA positive tumour cells [10]. However, it remains unclear whether BMs of lung cancer show PSMA staining and to what extent. In our research, PSMA was expressed not only in blood vessels but also in solid regions of BMs.

To investigate the expression of PSMA in solid regions of BMs, we implemented scRNA-seq analysis to quantify the expression level of PSMA. The results showed that PSMA was mainly expressed in oligodendrocytes infiltrating the BMs of lung cancer. In addition, we found

that PSMA overexpression was related to ER stress. ER stress has been well documented in many malignancies [27]. Tumour growth causes extreme changes in the microenvironment, including hypoxia, oxidative stress and glucose deprivation [28–30]. To survive, tumour cells must make internal and external adjustments, which in turn lead to the occurrence of ER stress and an increase in unfolded proteins [31–34]. Combined with the results of our study, we speculated that oligodendrocytes infiltrating into BMs of lung cancer led to ER stress, which was responsible for their high expression of PSMA.

When focusing on the mechanism of PSMA expression, the PSMA enhancer (PSME), a cis-element, was found to be involved in regulating the transcription and translation of PSMA in prostate cancers [35]. However, the mechanism by which PSMA expression is regulated in oligodendrocytes of BMs from lung cancer remains unclear. In our research, we noticed that the expression levels of the transcription factors ATF3 and NR4A1, which are related to ER stress, were significantly different when PSMA increased. The JASPAR website predicted that transcription factors ATF3 and NR4A1could bind to the promoter region of the folh1 gene and cause the overexpression of PSMA in oligodendrocytes in BMs.

According to the previous study in prostate cancer and glioblastoma, PSMA PET-CT in lung cancer have a potential application. Firstly, PSMA PET/CT might be a novel sensitive instrument to detect lung cancer associated with BMs, which is helpful to show the number, location, and size of BMs. Secondly, Although, mRNA and PSMA IHC data provide relevant information on PSMA expression levels, in clinical practice, the expression level of PSMA need to be detected by PSMA PET/CT to guide the eligibility for PSMA-RLT in lung cancer BMs. Furthermore, PSMA-targeted therapies have attracted many researchers to explore novel treatment approaches to cancers. Recently, PSMA antibody-drug conjugates (PSMA ADCs) have been applied for targeted therapy of cancer. Immunoglobulin G1 anti-PSMA monoclonal antibody was conjugated to monomethylauristatin E, bound to PSMA-positive cells and induced cytotoxicity [36]. As cellular immunotherapy has gained increasing momentum, chimeric antigen receptor (CAR)-T-cell therapy has become more widespread. CAR-T cells targeting PSMA have shown good results *in vivo* and are expected to achieve precision treatment of prostate cancer [37,38]. Targeted therapy for PSMA, including novel radioisotopes, immunotherapeutic ligands, and combined approaches, is expected to be useful in the treatment of lung cancer BMs.

However, it must be noted that our study is limited by the small sample size and single-centre experience. The results from scRNA-seq analysis cannot be fully representative of all BMs. Additional studies with large groups and multiple centre data are needed to assess the expression and application of PSMA in lung cancer associated with BMs.

5. Conclusion

In this study, we preliminarily investigated the clinical application of ^{68}Ga-PSMA PET/CT in lung cancer associated with BMs. Combined with the IHC and scRNA-seq analysis, the results indicated that PSMA was highly expressed in oligodendrocytes in BMs of lung cancer, and the expression of PSMA might be regulated by ATF3 and NR4A1, which are involved in ER stress and the unfolded protein response. PSMA might serve as a potential diagnostic, prognostic, and therapeutic target for lung cancer BMs.

Funding

This work was supported by the National Natural Science Foundation of China (No. 82103429 and 82173177), the Foundation of Shanghai Municipal Health Bureau (No. 20204Y0264). No other potential conflict of interest relevant to this article was reported.

Declaration of Competing Interest

The authors declare that there are no known conflicts of interest or personal relationships that could have appeared to influence the work reported in this paper.

Compliance with ethical standards

All patients involved in the study were reviewed and approved by the ethics committee of the Fudan University Shanghai Cancer Center.

CRediT authorship contribution statement

Yuchen Pei: Writing – original draft, Formal analysis. **Chang Liu:** Visualization. **Mingtao Feng:** Data curation, Formal analysis. **Liangdong Li:** Data curation, Formal analysis. **Changshuai Zhou:** Data curation, Formal analysis. **Lei Chen:** Data curation, Formal analysis. **Xin Hu:** Investigation, Project administration. **Shaoli Song:** Conceptualization, Formal analysis, Supervision. **Yiqun Cao:** Funding acquisition, Supervision. **Yang Gao:** Visualization, Supervision, Writing – review & editing.

References

[1] T.T. Lah, M. Novak, B. Breznik, Brain malignancies: glioblastoma and brain metastases, Semin. Cancer Biol. 60 (2020) 262–273, https://doi.org/10.1016/j.semcancer.2019.10.010.
[2] D.N. Cagney, A.M. Martin, P.J. Catalano, et al., Incidence and prognosis of patients with brain metastases at diagnosis of systemic malignancy: a population-based study, Neuro Oncol. 19 (2017) 1511–1521, https://doi.org/10.1093/neuonc/nox077.
[3] M. Alexander, S.Y. Kim, H. Cheng, Update 2020: management of non-small cell lung cancer, Lung 198 (2020) 897–907, https://doi.org/10.1007/s00408-020-00407-5.
[4] J.C. Evans, M. Malhotra, J.F. Cryan, C.M. O'Driscoll, The therapeutic and diagnostic potential of the prostate specific membrane antigen/glutamate carboxypeptidase II (PSMA/GCPII) in cancer and neurological disease, Br. J. Pharmacol. 173 (2016) 3041–3079, https://doi.org/10.1111/bph.13576.
[5] J.J. Vornov, K.R. Hollinger, P.F. Jackson, et al., Still NAAG'ing after all these years. The continuing pursuit of GCPII inhibitors, Adv. Pharmacol. 76 (2016) 215–255, https://doi.org/10.1016/bs.apha.2016.01.007.
[6] E. Nevedomskaya, S.J. Baumgart, B. Haendler, Recent advances in prostate cancer treatment and drug discovery, Int. J. Mol. Sci. 19 (2018) 1359–1383, https://doi.org/10.3390/ijms19051359.
[7] T. Maurer, M. Eiber, M. Schwaiger, J.E. Gschwend, Current use of PSMA-PET in prostate cancer management, Nat. Rev. Urol. 13 (2016) 226–235, https://doi.org/10.1038/nrurol.2016.26.
[8] Y. Gao, H. Zheng, L. Li, et al., Prostate-specific membrane antigen (PSMA) promotes angiogenesis of glioblastoma through interacting with ITGB4 and regulating NF-κB signaling pathway, Front. Cell Dev. Biol. 9 (2021), 598377, https://doi.org/10.3389/fcell.2021.598377.
[9] M. Kasoha, C. Unger, E.F. Solomayer, et al., Prostate-specific membrane antigen (PSMA) expression in breast cancer and its metastases, Clin. Exp. Metastasis 34 (2017) 479–490, https://doi.org/10.1007/s10585-018-9878-x.
[10] L.H. Schmidt, B. Heitkötter, A.B. Schulze, et al., Prostate specific membrane antigen (PSMA) expression in non-small cell lung cancer, PLoS One 12 (2017), e0186280, https://doi.org/10.1371/journal.pone.0186280.
[11] M.J.M. Uijen, Y.H.W. Derks, R.I.J. Merkx, et al., PSMA radioligand therapy for solid tumors other than prostate cancer: background, opportunities, challenges, and first clinical reports, Eur. J. Nucl. Med. Mol. Imaging 48 (2021) 4350–4368, https://doi.org/10.1007/s00259-021-05433-w.
[12] A.G. Wernicke, M.A. Edgar, E. Lavi, et al., Prostate-specific membrane antigen as a potential novel vascular target for treatment of glioblastoma multiforme, Arch. Pathol. Lab. Med. 135 (2011) 1486–1489, https://doi.org/10.5858/arpa.2010-0740-OA.
[13] J. Kunikowska, K. Bartosz, K. Leszek, Glioblastoma multiforme: another potential application for 68Ga-PSMA PET/CT as a guide for targeted therapy, Eur. J. Nucl. Med. Mol. Imaging 45 (2018) 886–887, https://doi.org/10.1007/s00259-018-3934-2.
[14] U. Haberkorn, M. Eder, K. Kopka, J.W. Babich, M. Eisenhut, New strategies in prostate cancer: prostate-specific membrane antigen (PSMA) ligands for diagnosis and therapy, Clin. Cancer Res. 22 (2016) 9–15, https://doi.org/10.1158/1078-0432.CCR-15-0820.
[15] W.P. Fendler, M. Eiber, M. Beheshti, et al., 68Ga-PSMA PET/CT: joint EANM and SNMMI procedure guideline for prostate cancer imaging: version 1.0, Eur. J. Nucl. Med. Mol. Imaging 44 (2017) 1014–1024, https://doi.org/10.1007/s00259-017-3670-z.

[16] N. Kim, H.K. Kim, K. Lee, et al., Single-cell RNA sequencing demonstrates the molecular and cellular reprogramming of metastatic lung adenocarcinoma, Nat. Commun. 11 (2020) 2285–2299, https://doi.org/10.1038/s41467-020-16164-1.
[17] R.E. Conway, N. Petrovic, Z. Li, W. Heston, D. Wu, L.H. Shapiro, Prostate-specific membrane antigen regulates angiogenesis by modulating integrin signal transduction, Mol. Cell. Biol. 26 (2006) 5310–5324, https://doi.org/10.1128/mcb.00084-06.
[18] R. Watanabe, M. Maekawa, T. Kiyoi, et al., PSMA-positive membranes secreted from prostate cancer cells have potency to transform vascular endothelial cells into an angiogenic state, Prostate 81 (2021) 1390–1401, https://doi.org/10.1002/pros.24237.
[19] R.E. Conway, K. Joiner, A. Patterson, et al., Prostate specific membrane antigen produces pro-angiogenic laminin peptides downstream of matrix metalloprotease-2, Angiogenesis 16 (2013) 847–860, https://doi.org/10.1007/s10456-013-9360-y.
[20] S.M. Schwarzenboeck, I. Rauscher, C. Bluemel, et al., PSMA ligands for PET imaging of prostate cancer, J. Nucl. Med. 58 (2017) 1545–1552, https://doi.org/10.2967/jnumed.117.191031.
[21] A. Holzgreve, A. Biczok, V.C. Ruf, et al., PSMA expression in glioblastoma as a basis for theranostic approaches: a retrospective, correlational panel study including immunohistochemistry, clinical parameters and PET imaging, Front. Oncol. 11 (2021), 646387, https://doi.org/10.3389/fonc.2021.646387.
[22] D.H. Simsek, S. Kuyumcu, F.Y. Agaoglu, S.N. Unal, Radionuclide therapy with 177Lu-PSMA in a case of metastatic adenoid cystic carcinoma of the parotid, Clin. Nucl. Med. 44 (2019) 764–766, https://doi.org/10.1097/RLU.0000000000002645.
[23] LH De Vries, L. Lodewijk, A.J.A.T. Braat, et al., ^{68}Ga-PSMA PET /CT in radioactive iodine-refractory differentiated thyroid cancer and first treatment results with 177 Lu-PSMA-617, EJNMMI Res. 10 (2020) 18–25, https://doi.org/10.1186/s13550-020-0610-x.
[24] A. Kumar, S. Ballal, M.P. Yadav, et al., ^{177}Lu-/68Ga-PSMA theranostics in recurrent glioblastoma multiforme: proof of concept, Clin. Nucl. Med. 45 (2020) E512–E513, https://doi.org/10.1097/RLU.0000000000003142.
[25] J. Czernin, R.C.D. Bolton, S. Ezziddin, F. Forrer, R.J. Hicks, EANM procedure guidelines for radionuclide therapy with ^{177}Lu-labelled PSMA-ligands (^{177}Lu-PSMA-RLT), Eur. J. Nucl. Med. Mol. Imaging 46 (2019) 2536–2544, https://doi.org/10.1007/s00259-019-04485-3.
[26] H.L. Wang, S.S. Wang, W.H. Song, et al., Expression of prostate-specific membrane antigen in lung cancer cells and tumor neovasculature endothelial cells and its clinical significance, PLoS One 10 (2015), e0125924, https://doi.org/10.1371/journal.pone.0125924.
[27] X. Chen, J.R. Cubillos-Ruiz, Endoplasmic reticulum stress signals in the tumour and its microenvironment, Nat. Rev. Cancer 21 (2021) 71–88, https://doi.org/10.1038/s41568-020-00312-2.
[28] M. He, W. Zhang, J. Wang, et al., Aggregative perivascular tumor cell growth pattern of primary central nervous system lymphomas is associated with hypoxia-related endoplasmic reticulum stress, J. Cancer 12 (2021) 3841–3852, https://doi.org/10.7150/jca.54952.
[29] K. Kalimuthu, J.H. Kim, Y.S. Park, et al., Glucose deprivation-induced endoplasmic reticulum stress response plays a pivotal role in enhancement of TRAIL cytotoxicity, J. Cell. Physiol. 236 (2021) 6666–6677, https://doi.org/10.1002/jcp.30329.
[30] Y. Lin, M. Jiang, W. Chen, T. Zhao, Y. Wei, Cancer and ER stress: mutual crosstalk between autophagy, oxidative stress and inflammatory response, Biomed. Pharmacother. 118 (2019) 109249–109258, https://doi.org/10.1016/j.biopha.2019.109249.
[31] S.A. Oakes, Endoplasmic reticulum stress signaling in cancer cells, Am. J. Pathol. 190 (2020) 934–946, https://doi.org/10.1016/j.ajpath.2020.01.010.
[32] S.W. Xia, Z.M. Wang, S.M. Sun, et al., Endoplasmic reticulum stress and protein degradation in chronic liver disease, Pharmacol. Res. 161 (2020), 105218, https://doi.org/10.1016/j.phrs.2020.105218.
[33] K. Miyazaki, S. Inoue, K. Yamada, et al., Differential usage of alternate promoters of the human stress response gene ATF3 in stress response and cancer cells, Nucleic Acids Res. 37 (2009) 1438–1451, https://doi.org/10.1093/nar/gkn1082.
[34] C. Yu, S. Cui, C. Zong, et al., The orphan nuclear receptor NR4A1 protects pancreatic β-cells from endoplasmic reticulum (ER) stress-mediated apoptosis, J. Biol. Chem. 290 (2015) 20687–20699, https://doi.org/10.1074/jbc.M115.654863.
[35] W. Peng, L. Guo, R. Tang, et al., Sox7 negatively regulates prostate-specific membrane antigen (PSMA) expression through PSMA-enhancer, Prostate 79 (2019) 370–378, https://doi.org/10.1002/pros.23743.
[36] W.P. Fendler, K. Rahbar, K. Herrmann, C. Kratochwil, M. Eiber, ^{177}Lu-PSMA raDioligand therapy for prostate cancer, J. Nucl. Med. 58 (2017) 1196–1200, https://doi.org/10.2967/jnumed.117.191023.
[37] F. Wang, Z. Li, X. Feng, D. Yang, M. Lin, Advances in PSMA-targeted therapy for prostate cancer, Prostate Cancer Prostatic Dis. 25 (2022) 11–26, https://doi.org/10.1038/s41391-021-00394-5.
[38] C.C. Kloss, J. Lee, A. Zhang, et al., Dominant-negative TGF-β receptor enhances PSMA-targeted human CAR T cell proliferation and augments prostate cancer eradication, Mol. Ther. 26 (2018) 1855–1866, https://doi.org/10.1016/j.ymthe.2018.05.003.